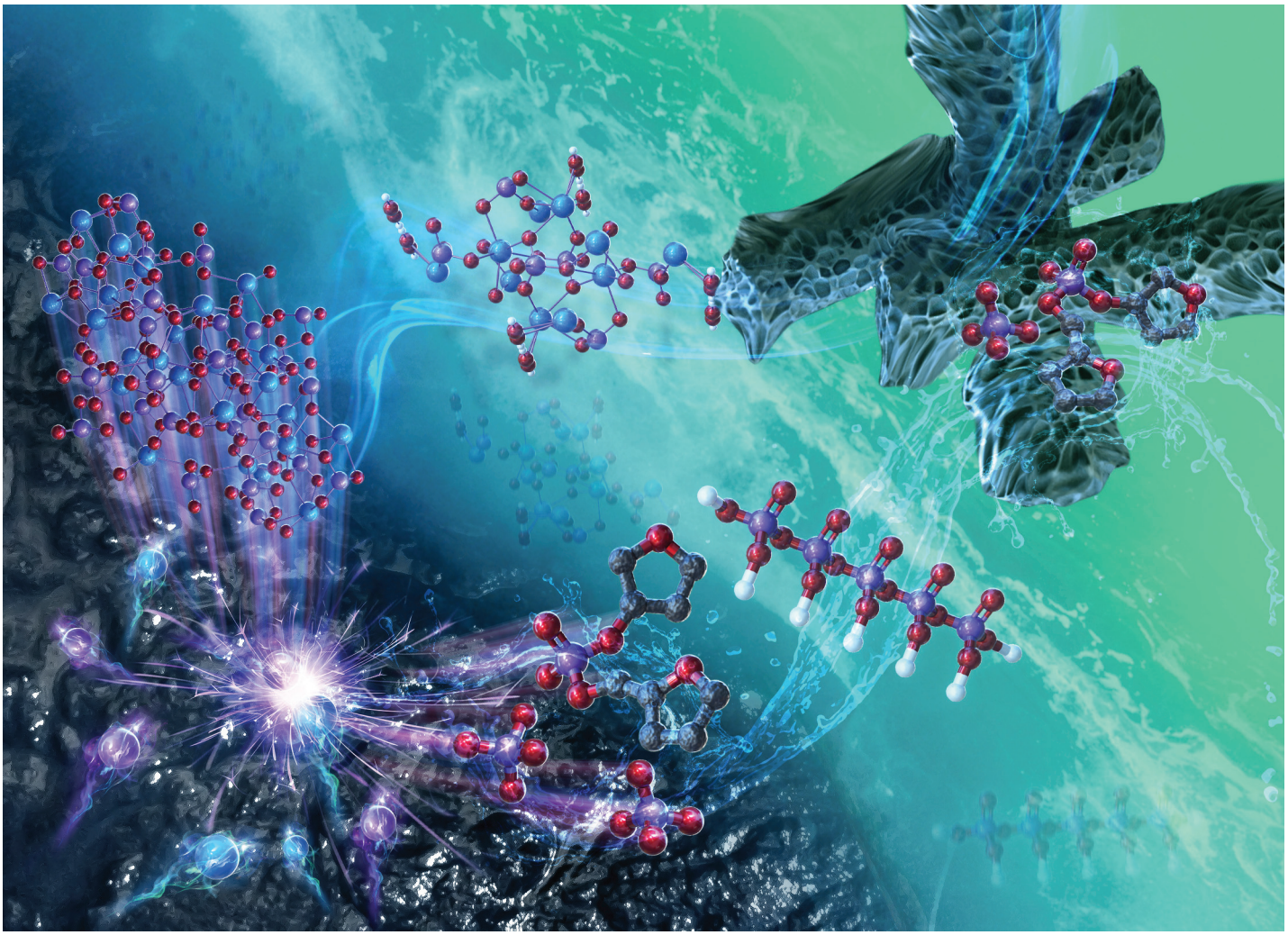

An article presented by Associate Professor Tao Zhang from China Agricultural University, China and Professor James Clark from University of York, UK.

Mechanisms and modelling of phosphorus solid–liquid transformation during the hydrothermal processing of swine manure

Phosphorus recovery from swine manure by hydrothermal processes has recently attracted a considerable interest. Here, transformation mechanisms and distribution modelling of soluble and in-soluble phosphate from the swine manure were investigated during hydrothermal processes. The findings could offer a range of scientific opportunities for a comprehensive understanding of the basis of sustainable utilisation of phosphorus.

As featured in:

See Tao Zhang *et al.*, *Green Chem.*, 2020, **22**, 5628.

ROYAL SOCIETY OF CHEMISTRY

rsc.li/greenchem

Registered charity number: 207890

Green Chemistry

PAPER

Cite this: *Green Chem.*, 2020, **22**, 5628

Mechanisms and modelling of phosphorus solid–liquid transformation during the hydrothermal processing of swine manure

Yaxin Deng,†[a] Tao Zhang, *†[a] James Clark, [b] Tejraj Aminabhavi,[c] Andrea Kruse,[d] Daniel C. W. Tsang, [e] Brajendra K. Sharma, [f] Fusuo Zhang[a] and Hongqiang Ren[g]

Received 11th April 2020,
Accepted 18th June 2020

DOI: 10.1039/d0gc01281e

rsc.li/greenchem

Phosphorus (P) recovery from swine manure by hydrothermal processes has recently attracted considerable interest; however, research has been limited by knowledge gaps and challenges in understanding the mechanisms of soluble and insoluble P transformations and the evaluation of the effects of the reaction conditions. In this study, the transformation mechanisms were investigated and the soluble and insoluble phosphorus distributions in swine manure during the hydrothermal processes were modelled. By increasing the severity of the exogenous conditions, P transformed from insoluble to soluble, and then polymerized with the formation of orthophosphates; meanwhile, the formation of hydrochar was enhanced thereby facilitating further P reclamation. The effects of the endogenous conditions showed there may be a threshold of calcium content, which limited the combination of Ca and P. Calcium ions mainly reacted with P in the form of hydroxyapatite and octacalcium phosphate. The modelling and prediction results showed that a coalification model gives a good fit (R_{SP}^2 = 0.9205 and R_{IP}^2 = 0.8559) for changes in the concentrations of solid total P and liquid inorganic P. The prediction level of mean absolute error was good as well (MAE_{SP} = 0.74 mg g^{-1} and MAE_{IP} = 0.62 mg g^{-1}). These findings provide a range of scientific opportunities for achieving a comprehensive understanding of the basis of sustainable utilisation of P.

Introduction

With the increasing growth of the global population, concentrated animal feeding operations have accelerated worldwide, leading to the production of a tremendous amount of manure. This manure generally contains high levels of organic matter, which is responsible for its characteristic odour as well as pathogens, hormones, pharmaceutically derived compounds, and metal salts, such as Cu, Fe, Mg, Ca and Al.[1,2] However, animal manure also provides a promising renewable source of nutrients for recycling, such as phosphorus (P), nitrogen (N), potassium, and other micronutrients.[3]

Traditionally, animal manure management has involved its application to farmland as fertiliser with or without simple pre-treatments, such as composting, lime treatment, or alum treatment.[4] However, this results in eutrophication and causes human and environmental hazards because of the embedded organic contaminants (*e.g.*, antibiotics and pesticides). Since manure is regarded as a "renewable secondary P resource",[5] there would be challenges in sustainable waste management to minimise the hygienic and ecological risks connected with the utilisation of animal manure, meanwhile maximising the P recovery.

Recently, hydrothermal methods have shown promise for the treatment of moisture-rich animal manure because of their high tunability when used to convert solid biowaste into products with broad applications (hydrochar, fuel, and organic products).[1,6] Despite the dominance of hydrothermal routes as techniques for resource recovery, few studies have investigated P recovery from manure during hydrothermal processing. Dai *et al.* (2015) used hydrothermal carbonization as a method for manure management to achieve P reclamation in hydrochar.[7] Ekpo *et al.* (2016) investigated the effects of pH on P extraction

[a]*Beijing Key Laboratory of Farmland Soil Pollution Prevention and Remediation, Key Laboratory of Plant-Soil Interactions of Ministry of Education, College of Resources and Environmental Sciences, China Agricultural University, Beijing 100193, China. E-mail: taozhang@cau.edu.cn*
[b]*Green Chemistry Centre of Excellence, University of York, Heslington, York, YO10 5DD, UK. E-mail: james.clark@york.ac.uk*
[c]*College of Pharmacy, Dharwad, India. E-mail: aminabhavit@gmail.com*
[d]*Institute for Agricultural Engineering, University of Hohenheim, Garbenstrabe 9, 70599 Stuttgart, Germany*
[e]*Department of Civil and Environmental Engineering, The Hong Kong Polytechnic University, Hung Hom, Kowloon, Hong Kong, China*
[f]*Illinois Sustainable Technology Center, Prairie Research Institute, University of Illinois, Urbana-Champaign, 1 Hazelwood Drive, Champaign, IL 61820, USA*
[g]*State Key Laboratory of Pollution Control and Resource Reuse, School of the Environment, Nanjing University, Nanjing 210093, Jiangsu, China*
†These authors contributed equally to this work.

from swine manure after hydrothermal treatment and found that the presence of acidic additives improved nutrient extraction.[1] However, most studies performed to date have focused on the optimisation of process parameters and technical routes, which may be invalid when conditions vary.[8]

Previous studies have shown that the speciation and contents of metal ions with strong affinities for P in the biomass affect the recovery efficiency and bioavailability of P.[9] Heilmann *et al.* (2014) found that multivalent metal cations (Al, Ca, Mg, and Fe) are the controlling factors which lead to the formation of insoluble phosphates in hydrochars.[2] Therefore, it is necessary to investigate the reaction mechanisms of soluble and insoluble phosphate formation during the hydrothermal processes to boost the efficiency of P recovery under different hydrothermal conditions. Huang and Tang (2016) summarised the mechanisms of phosphate precipitation in different types of biowastes and the controlling factors (*i.e.* treatment techniques and conditions), but their findings were largely limited to qualitative descriptions.[9] To the best of our knowledge, no systematic study has yet been performed to investigate the transformation and reclamation mechanisms associated with P in the hydrothermal processes or for the quantitative analysis of the effect of the reaction conditions on the solid–liquid distribution of P from animal manure.

The principal objectives of the present study were to quantify the external factors (temperature and time) affecting the hydrothermal treatment of manure by using a severity factor model, investigate the effect of the reaction severity and an internal factor (Ca^{2+}) on the P solid–liquid distribution, transformation, and reclamation, and set up a mathematical modelling approach for predicting the P solid–liquid distribution. It is worth noting that this study is the first of its kind to use the coalification approach and other empirical models to fit and predict the P solid–liquid distribution.

Results and discussion

Influence of exogenous factors

Influence on the solid–liquid distribution of phosphate. Temperature and residence time both had significant effects on P transformation during the hydrothermal process. Some previous studies showed that the effects of temperature and time on the hydrothermal reaction were equivalent to some extent.[10] Thus, to have a better comparison of experimental results under different conditions, we introduced the severity factor to correlate the effects of operation conditions (temperature and residence time). The severity factor was proposed by Overend and Chornet (1987), by modeling the effects of the main operational variables by pseudo first-order kinetics.[11] It enabled a deeper insight into several phenomena involved and provided mathematical equations suitable for simulation, optimization and the design of operational strategies.[12] The severity factor had been developed by a number of authors for different hydrothermal processes. Here we chose the adjusted severity factor (eqn (4)) by Jung and Kruse (2017).[13] For simplicity, we used $\mathrm{Ln}(R_0)$ as the reaction variable. Fig. 1a and b show the P concentrations in liquid and solid states during different reactions ($\mathrm{Ln}(R_0)$). Here, we chose inorganic-P to represent liquid-P because it has more applications as a resource, thus, the quantitative analysis of inorganic-P may be useful for P recovery industries, and we also performed a qualitative analysis for aqueous organic-P, as described in the following section. In addition, mg g^{-1} was chosen as the unit of liquid-P for a better comparison of liquid-P and solid-P.

The concentrations were modelled appropriately by the cubic function ($R_{\mathrm{liquid}}^2 = 0.6706$ and $R_{\mathrm{solid}}^2 = 0.7220$). The inorganic-P (soluble-P) yield initially increased, and then decreased with increasing reaction severity. The solid-P (insoluble P) yield showed the opposite trend. There were two major stages in the P transformation process. During the first stage, at the severities of 7.7–11.0, the yield of soluble-P increased (Fig. 1a), but the rate of increase gradually decreased until reaching zero at a severity of 11.0. These findings were confirmed by the first derivatives (concentration divided by time) of the soluble phosphorus (Fig. 1c), which showed the variations in the soluble phosphorus yield rate. The variations in the insoluble phosphorus yield were almost the opposite of those for soluble phosphorus during the first stage (Fig. 1b). During the second stage, the soluble phosphorus yield decreased and that of insoluble phosphorus increased after a severity of 11.0 was reached, but the formation rates were slow (Fig. 1c and d).

At the beginning of the hydrothermal process, hydrolysis of large organic phosphorus released phosphate into the aqueous environment. These macromolecular organic compounds include phytates, polyphosphates, phosphate monoesters, and phosphate diesters.[9] The transformation of insoluble organic-P into soluble organic-P may have been enhanced by dehydration. During this stage, much inorganic-P was released; however, the inorganic-P content in the system decreased at the same time. Heilmann *et al.* (2014) found that the presence of multivalent cations of metals such as aluminium, calcium, magnesium, and iron can lead to the formation of insoluble phosphates in colloidal forms or electrostatically attached to proteins in manure.[2] Moreover, hydrochar can decrease the inorganic-P content in the aqueous phase by trapping it. Wiedner *et al.* (2013) showed that hydrochars produced during hydrothermal carbonisation had a nutrient retention capacity.[14] This indicates that the decrease in the amount of inorganic-P in the liquid may be caused by the adsorption on hydrochar. By increasing the reaction severity (a parameter indicating the synthetic thermal effect of temperature and pressure), the decrease in inorganic-P in the aqueous phase was strengthened. At higher severity, degradation of polyphosphate produced increasing amounts of short-chain polyphosphates, which created additional P–O bonds for metal complexation.[9] At the same time, the presence of negatively charged oxygen-containing functional groups such as carboxylate and hydroxyl functional groups, which can coordinate with metal ions, reportedly decreased with increas-

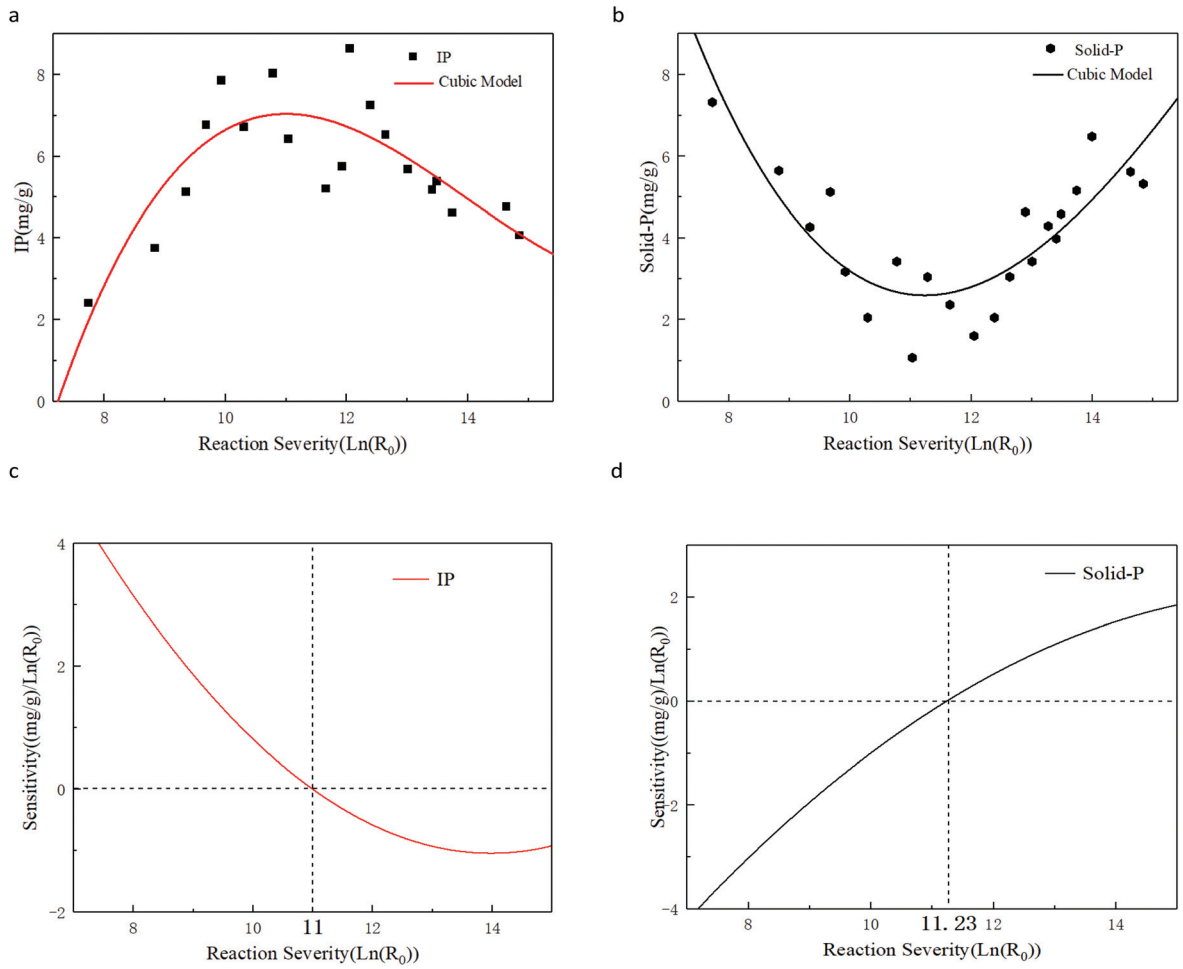

Fig. 1 Inorganic-P and solid-P yields (a and b), and derivative and second derivative (c and d) at different reaction severities.

ing reaction severity.[15] This indicates that more free metal ions were released. Both factors facilitate the combination of metal ions and P.

Influence on the transformation of soluble phosphorus. The transformation of P forms in a hydrothermal aqueous system is important for subsequent recycling and reuse of P. Therefore, ^{31}P liquid Nuclear Magnetic Resonance (NMR) was used to identify the P forms in the aqueous system under different hydrothermal conditions (Fig. 2). According to Cade-Menun (2005), the P forms in raw manure were primarily orthophosphates (4.88 ppm) and orthophosphate diesters (0.85 ppm and −0.95 ppm).[16] The number of P forms extracted from raw manure was small, and the concentrations were low. There are two reasons for this phenomenon. The coupled chemical extraction (NaOH-EDTA) and ^{31}P liquid NMR method can only identify the P forms solubilised into the extractant solution, and this method may cause alteration to P complexation forms or the hydrolysis of organic-P.[17] It is possible that most of the P in the raw manure was in the solid state and trapped in mineral crystal lattices. Along with the increase in reaction thermal severity (Ln(R_0)) from 12.14 to 15.00, the number of P forms might have increased and then decreased. At a reaction severity of 12.14, there was a significant signal from orthophosphate diesters (2.58 ppm), including phospholipids and DNA,[16] which indicates that the insoluble organic-P was transformed into a soluble form by hydrothermal treatment. Compared to raw manure, the signal of orthophosphate (4.88 ppm) disappeared, and the concentrations of orthophosphate diesters increased. As the severity increased, more P-absorbed sites were created, transferring the orthophosphate into hydrochar. These findings are consistent with the findings reported in section Influence on the solid–liquid distribution of phosphate, and show a decrease in inorganic-P in the aqueous phase after reaching a severity of 11.00.

When the severity was 12.18, the P forms increased, indicating more insoluble organic-P was depolymerised into the soluble form, namely phosphonate (18.43 ppm) and orthophosphate diester (2.53 ppm and 0.83 ppm). When the severity of the reaction was increased, decarbonisation resulted in increased dissolution of short-chain organic-P in the aqueous phase. This was confirmed by the presence of orthophosphates at 0.83 ppm. Moreover, repolymerisation of short-chain organic-P produced long-chain organic-P. This was confirmed by the presence of a phosphonate signal at 18.43 ppm. As the

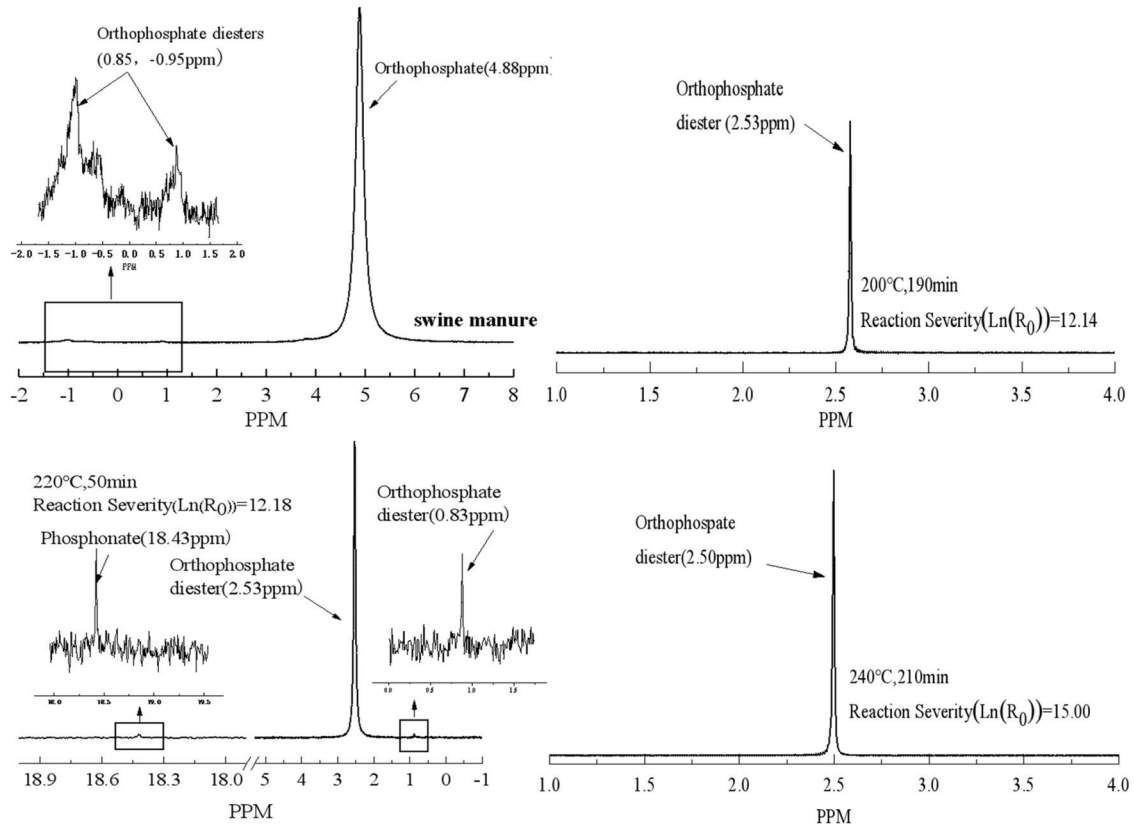

Fig. 2 ^{31}P NMR spectra of a range of samples.

reaction proceeded, the number of forms of P decreased and only orthophosphate diesters (2.50 ppm, Ln(R_0) = 15.00) remained in the supernatant. These findings confirmed the previous findings that indicated regardless of the types of feedstocks and initial P forms, hydrothermal treatment generally homogenized all of the P forms into single form,[7] which was useful for P reclamation.[18]

Influence on phosphorus reclamation. The ^{31}P NMR spectra facilitated the identification of the forms of P in the aqueous system, but did not provide structural information on hydrochar, which also plays an important role in the migration and stability of P in the system. The X-ray Powder Diffraction (XRD) patterns of untreated and hydrothermally treated samples are shown in Fig. 3. The XRD diffraction peaks for the swine manure were broad, and there were still some peaks at 2θ values of 15–20° and 25–34°, which represented the microcrystalline cellulose structures.[19] The XRD profiles suggest a complex blend of crystalline and amorphous phases, characterised by narrow and intense peaks superimposed on a large and low intensity peak. After 190 min of 200 °C hydrothermal carbonisation (HTC) treatment, the XRD curve peaked at 2θ values of 25–60° and is sharper than those of swine manure (Ln(R_0) = 12.14), indicating the formation of calcium salts in various structures.[20] At the same time, the cellulose peaks clearly dropped, indicating the increase in reaction severity destroying the crystallinity of cellulose. Moreover, the crystallisation increased in hydrochar, indicating the degradation of amorphous components of swine manure (*e.g.*, hemicellulose, extractives, and amorphous cellulose).[21] These findings suggest that the feedstock solubilisation and hydrochar formation at 200 °C were mainly caused by the degradation of amorphous components. As the reaction severity increased, the peaks between 35° and 60° almost disappeared (Ln(R_0) = 12.18, 15.00), while the presence of a broad peak between 20° and 30° became more obvious, indicating the formation of amorphous carbon.[22] Additionally, the synthesised hydrochars were composed of disordered and amorphous structures, which is consistent with the results of previous studies.[21,23,24] This suggests that a low reaction severity has a positive effect on crystallisation, but when the reaction severity increases, crystallisation might have been destroyed to enhance the formation of amorphous carbon. Furthermore, P reclamation may have been facilitated by the increase in reaction severity because of the adsorption of P by the porous hydrochar.

Influence of endogenous conditions (Ca^{2+})

Influence on the solid–liquid distribution of phosphate. P partitioning into solid and liquid phases has been shown to be determined not only by the treatment conditions, but also by the interplay between feedstock characteristics, especially for the feedstock with high salt contents that generally result in more P retention in the solid hydrochars.[1,25] For instance,

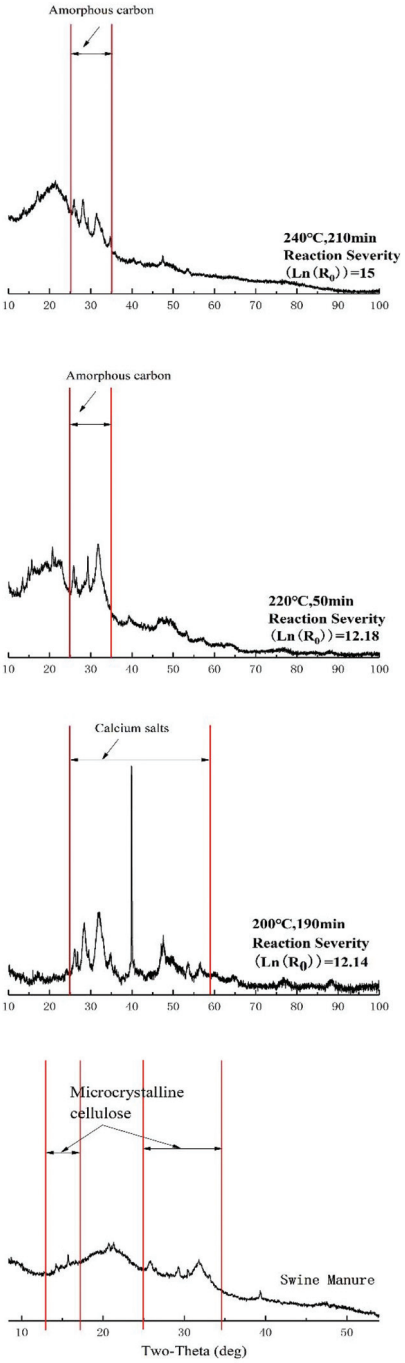

Fig. 3 XRD curves of raw manure and hydrochars at different reaction severities.

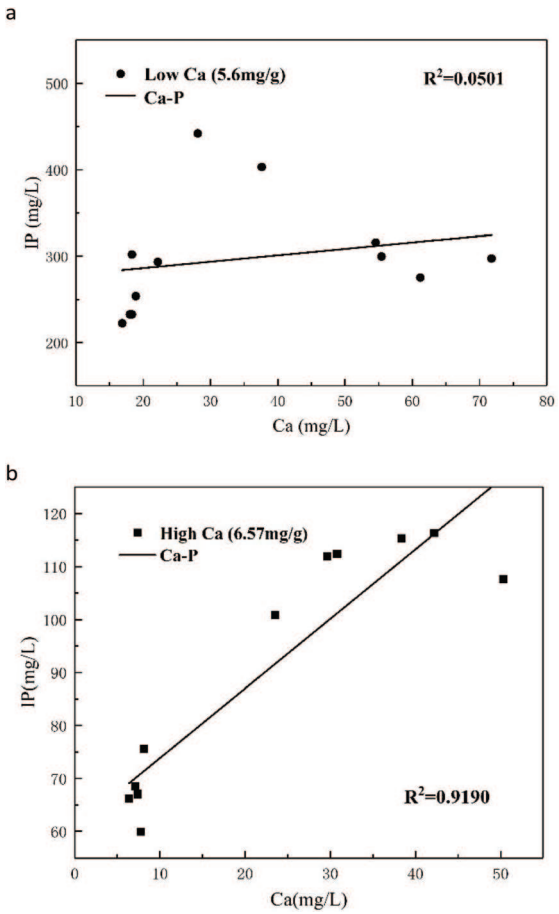

Fig. 4 The correlation between calcium and inorganic-P at different calcium contents: (a) 5.60 mg g^{-1} and (b) 6.57 mg g^{-1}.

metals ions such as Ca, Mg, Cu, and Zn can form insoluble phosphate precipitates, and Fe and Al (hydr)oxide minerals have affinities for P adsorption. Among these metal cations, calcium became a key factor capturing P in hydrochar because of its high content in swine manure and had high affinities for P to form precipitates and/or surface complexes.[26] Hence, Ca^{2+} is an important factor influencing P liquid–solid distribution.

As shown in Fig. 4a, it was difficult to find a significant correlation (R^2 = 0.0501) between the Ca ion input and soluble phosphate in the aqueous phase when the raw manure was treated by hydrothermal carbonisation (Ca^{2+}: 5.6 mg g^{-1}, solid content 4.1%) at 200 °C. This was different from the results of previous studies showing there was a high correlation (R^2 > 0.9) between Ca^{2+} and soluble phosphate.[6,27] According to the previous studies, cations were found to be in insufficient quantity for the formation of significant quantities of insoluble phosphates that could be incorporated into hydrochars, when its concentrations were low (less than 0.5%).[28] The threshold value (0.5%) may not be precise due to the differences of raw materials and other related factors. But it indeed showed that phosphorus may not react with multivalent metal ions when it is insufficient. To confirm the concentration of Ca, which is a key factor controlling the reaction of calcium phosphate, we increased the total calcium ion concentration to 6.6 mg g^{-1} in the system with 20 mg L^{-1} $CaCl_2$ solution. As shown in Fig. 4b, a high correlation emerged between Ca and P with an R^2 = 0.9190, which showed that the concentration of metal ion was a key factor, and also it confirmed that there may be a threshold of calcium content limiting the combination of Ca and phosphorus, below which it is difficult to form significant quantities of insoluble phosphates in hydrochars. However, the threshold value is highly correlated to the

practical conditions, thus we performed a qualitative analysis in this study.

To investigate further, variations in the soluble inorganic-P, soluble-Ca and solid-Ca concentrations in different reaction stages (retention time: 50, 70, 90, 190, 210, and 230 min; temperature, 200 °C; Ca^{2+}, 6.57 mg g^{-1}) were plotted (Fig. 5). Under the conditions of high calcium ion concentration (6.57 mg g^{-1}), the metal cation was not able to capture the phosphate during the initial stage of the reaction. When the retention time was increased to 90 min, the formation of insoluble Ca–P salts became more significant, and the concentration of inorganic-P and Ca in the aqueous phase decreased sharply. After 190 min, the concentrations of solid-Ca became stable, indicating that the formation of insoluble Ca–P salts tended to stabilise.

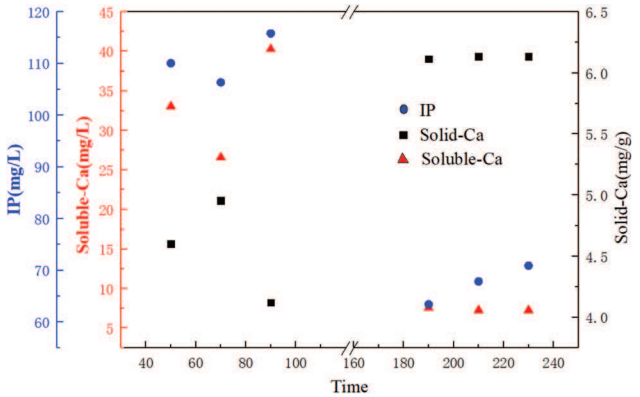

Fig. 5 Variations of inorganic-P, Ca and solid-Ca concentrations in different reaction stages.

This could be due to the fact that during the initial stage, some labile organic matter containing carboxyl and hydroxyl groups may have coordinated with Ca to hinder the contact between Ca and P, thus preventing the formation of insoluble Ca–P compounds.[29] In any case, increase of retention time led to the formation of recalcitrant aromatic carbon. Aromatic structures exhibited high stability under the hydrothermal conditions,[10] with a few carboxyl and hydroxyl groups and consequently exhibited little effect on the reaction between Ca and P. The formation of insoluble Ca–P compounds therefore increased significantly.

Influence on phosphate reclamation. In order to investigate the precipitation of calcium phosphates further, the crystalline structure covering the surface of hydrochar in different treatments was analysed by XRD. As shown in Fig. 6, the XRD patterns of hydrochar from different Ca concentration inputs were compared. The samples showed similar curves, except that there was a new peak in the XRD curves of low Ca

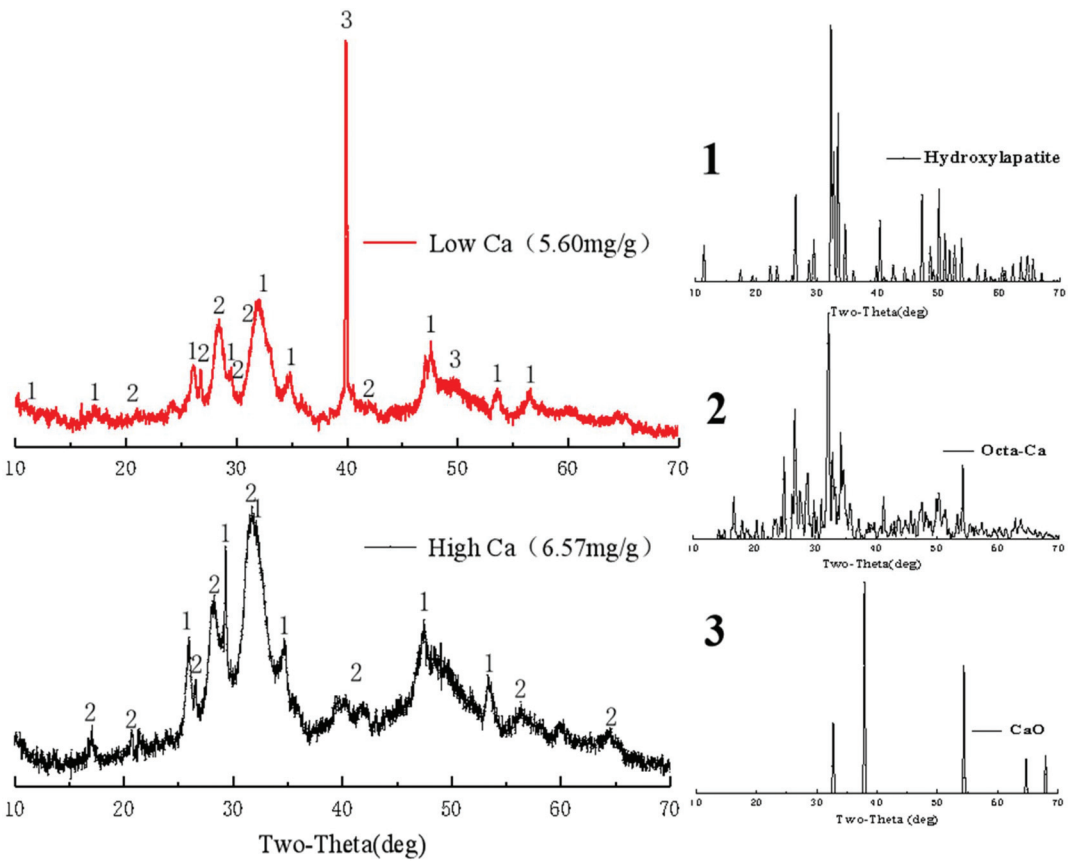

Fig. 6 XRD curves of hydrochars at different Ca concentrations for 190 min at 200 °C.

concentrations. These results showed that there were two P-containing minerals in both kinds of samples; namely, hydroxylapatite and octa-Ca. It must be pointed out that the peak area of hydroxylapatite and octa-Ca did not change a lot at different Ca concentrations. There are mainly two reasons for that. One is that XRD is a qualitative analysis method, the peak areas are a comparative characterization of crystal contents, so it is not an accurate way to equate the peak area to the crystal content. The other one is that the peak area is influenced by the positions and angles of radiations, which cannot be controlled. Therefore, the peak area cannot be an indicator of crystal content changes.

Additionally, the new peak observed in the low Ca^{2+} sample indicated that there was CaO in the sample (Fig. 6). These findings show that when the content of Ca was low in the aqueous phase, it could not combine with phosphorus; therefore, Ca ions formed CaO. However, when the cation concentration increased (high Ca^{2+} content), the Ca ions in the system were sufficient to form Ca-phosphate. From the abovementioned results, we can make a conclusion apparently, namely, under the same external conditions, the higher Ca concentration promotes the transformation of phosphorus from liquid to solid.

Modelling and prediction

Given the variations in the raw materials and diversity of equipment, it is necessary to construct a model connecting the input and output variables for pilot or industrial scale P-recovery plants. In this study, mathematical evaluation was conducted based on the hydrothermal carbonisation experimental data to identify the optimal process conditions and predict output streams. The dataset consisted of three parts, namely the results from the reaction condition experiments, experiments in which samples containing different solid contents (1.025%–8.2%) were treated at 200 °C for 30, 70, 110, and 150 min, and experiments performed at different reaction temperatures, ranging from 90 °C to 260 °C, with retention times of 10 min to 70 min and solid ratios of 6% to 10%. The characteristics of feedstock used are shown in Table 1.

Modelling soluble and non-soluble phosphate. The performances of the models were evaluated for the temperature range of 180 °C–240 °C, retention times of 10–210 min, and solid ratios of 1.03%, 2.05%, 4.10%, and 8.20%. The correlation values for different models are shown in Table 2. For P partitioning, the coalification model gave the highest correlation values for insoluble (P_{solid}) and soluble phosphate ($P_{inorganic}$)

Table 1 The characteristics of feedstock

Parameter	Value (%)
TKN	2.63
P	2.59
Ca	1.80
Mg	1.04
Al	0.05
Fe	0.27
Moisture	3.23

Table 2 The fit-correlation values of different models

	Coalification	Linear regression	Severity factor	Dose–response
Solid-P	0.9205	0.8954	0.8669	—
PO_4^{3-}	0.8559	0.8466	0.7997	0.8321

among these four models (R^2 = 0.9205 and 0.8559, respectively), which can be described by two equations: eqn (1) and (2).

$$P_{solid} = \ln(108.55) - 0.94\ln(t) - \frac{725.88}{T} + 176.53S, \quad (1)$$

$$P_{inorganic} = \ln(661.76) + 0.73\ln(t) - \frac{73.19}{T} - 101.70S. \quad (2)$$

These equations describe the behaviour and contributions of time, temperature and solid ratio on the P distribution. The solid ratio and retention time played positive roles for the P_{solid} yield; meanwhile, they had negative effects on $P_{inorganic}$ yield. Moreover, higher temperature was found to promote phosphate transformation. In Fig. 7, different colours indicate

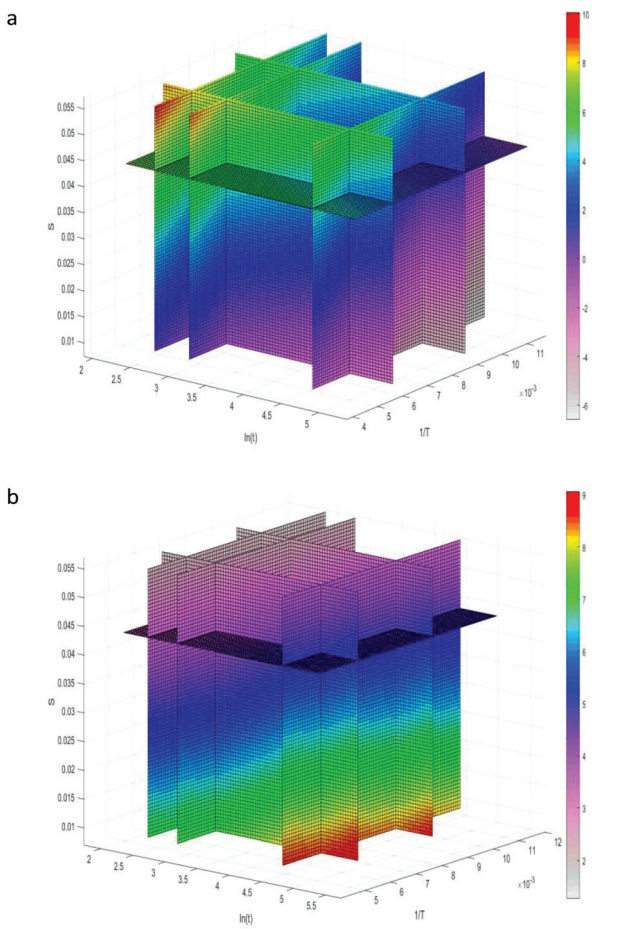

Fig. 7 The coalification models of insoluble solid-P (a) and soluble inorganic-P (b).

different concentrations of insoluble solid-P (Fig. 7a) and soluble inorganic-P (Fig. 7b), with colours changing from light to dark, indicating the concentration change from low to high concentrations. Based on the values of the coefficients of different parameters, both equations indicate that the temperature and solid ratio were more important than the retention time in the P solid–liquid distribution. The concentrations of intermediate compounds in the liquid phase may increase more quickly and the polymerisation reaction may start earlier at lower biomass/water ratios;[30] however, low solid ratios would inhibit further conversions, which explains why a high solid ratio favoured the formation of insoluble rather than soluble P.[10]

Prediction based on the coalification model. The coalification model was applied to determine how accurate its predictions were compared with the measured data. The predictions were evaluated based on the mean absolute error (MAE) by using the experimental data collected from 29 hydrothermal treatment runs for another type of swine manure. The reaction temperature ranged from 90 °C to 260 °C, while the time ranged from 10 to 70 min, and the solid ratio from 6% to 10%. As shown in Table 3, application of the coalification model to the solid-P and inorganic-P in the aqueous phase resulted in a MAE of 0.74 and 0.62 mg g^{-1}, respectively, indicating the coalification model had a good ability to model the hydrothermal process.

It should be noted that the coalification model had some limitations. For instance, there were no lower or upper boundaries in the equations, and the optimised values could not be restricted to a reasonable range. Hence, to some extent, the model was more suitable for the prediction than optimisation. Additionally, the coalification model was a lumped equation, in contrast to kinetic equations, which require monitoring of certain intermediates and structural quantities.[31] Moreover, the developed model cannot distinguish between areas in which the catalytic effect of subcritical water did and did not occur, indicating this approach cannot describe changes in the reaction mechanisms.[13]

For hydrothermal carbonisation, there are two reaction pathways, which describe the formation of primary and secondary chars.[32] Secondary char formation is a homogeneous reaction based on the hydrolysis products of polysaccharides and the polymerisation or condensation of dehydration products.[33] In contrast, primary char formation is a heterogeneous solid-to-solid conversion, which results in growth from a nucleus to hydrochar.[13] As discussed in the sections "Influence of exogenous factors" and "Influence of endogenous conditions (Ca^{2+})", soluble inorganic-P was produced by the hydrolysis and dehydration of P-containing macromolecules, and the formation of primary char occurred during the initial stage, which had something in common between these two processes. Both of these processes are hydrolysis reactions which release small molecules or ions. For the re-formation of insoluble solid-P, adsorption and precipitation are important in secondary char formation. Moreover, the formation of insoluble phosphates occurs on a time scale, similar to that of secondary char formation. Hence, the challenge in mathematically describing the hydrothermal process was determining whether it undergoes a primary or secondary char formation. Some studies have shown that the transformation of hemicellulose, cellulose and lignin fractions was related to the reaction process.[10,34]

Innumerable other studies on their behaviours during the hydrothermal processes have been conducted to reveal the reaction mechanisms. Lignin has a very low reactivity under hydrothermal conditions, although mass reduction and secondary char formation have been observed.[19] In addition, Dinjus and Kruse (2011) found that the crystallinity of cellulose reduced the hydrolysis rate.[35] Therefore, Lynam *et al.* (2012) introduced a new variable to quantify structural changes with the reactivity index ((fibre fraction of hemicellulose + solubles)/(lignin + ash)).[36] This reactivity index will be introduced to improve the accuracy of our model in future studies.

Table 3 MAE for the predicted concentrations of solid-P and inorganic-P

P state	Samples	MAE (mg g^{-1})
Inorganic-P	23	0.62
Solid-P	6	0.74

Experimental

Materials

The swine manure used in this study was collected from the Illinois Sustainable Technology Center (1 Hazelwood Drive, Champaign, IL, USA). The manure was pre-dried in an oven at 60 °C for several days, after which it was ground into powder (<2 mm). The ultimate analysis was performed using a CE Instruments Flash EA 1112 series elemental analyser to determine the weight percentage (wt%) of nitrogen and sulphur. Proximate analysis was performed using a thermogravimetric analyser (TGA) to determine moisture. Total P, Ca, and Mg were digested using H_2O_2–H_2SO_4 and analysed using an inductively coupled plasma-atomic emission spectrometer (ICP-AES; Optima 7300DV, PerkinElmer, Boston, MA, USA). All measurements were performed in duplicate and the mean values were reported. The chemical characteristics of the manure samples are shown in Table 4.

Table 4 Chemical characteristics of the swine manure sample

Parameter	Value (%)
N	1.44
S	0.13
P	1.01
Ca	0.56
Mg	0.20

Hydrothermal processing

Hydrothermal carbonisation of swine manure was performed in an unstirred 10 mL, high-pressure batch reactor. Manure slurry was diluted to different solid contents (1.03%, 2.05%, 4.10% and 8.20%) with deionised water. In each experiment, to explore the influences of reaction conditions (temperature and time), the reactor was charged with 5 ml diluted manure slurry (solid content, 4.1%) and then sealed and heated in an oven at 180 °C, 200 °C, 220 °C, and 240 °C. At each temperature stage, the retention time was set at 10–210 min. To reveal the calcium phosphate formation, experiments with different calcium contents (Ca: 5.6 and 6.6 g kg^{-1}, solid content: 4.1%) were conducted at 200 °C for 50–230 min.

Analysis of hydrochar and aqueous products

The total P in aqueous samples was analysed as per the standard methods.[37] PO_4-P in aqueous samples was also measured by the standard method (APHA, 2012, 4500-PC vanadomolybdophosphoric acid colorimetric method) after filtration through a 0.45 μm syringe filter.[37] The calcium ions in aqueous samples were determined using atomic absorption spectroscopy (900T, PerkinElmer, Boston, MA, USA).

^{31}P liquid nuclear magnetic resonance analysis. To trace the P speciation dynamics during the hydrothermal process, the supernatant from different reactions was analysed by liquid ^{31}P NMR. The supernatant products were lyophilised and concentrated by 10 times with 0.25 M NaOH/0.05 M EDTA. For P speciation in the raw swine manure, dry samples (0.5 g) were immersed in 10 mL of 0.25 mol L^{-1} NaOH + 50 mmol L^{-1} EDTA in 15 mL centrifuge tubes, and then shaken for 24 h using an end-over-end shaker at 298 K. Next, the samples (0.5 g dry samples with 10 ml solvent for each) were centrifuged (Avanti JXN-30, Beckman Coulter, USA) for 20 min.

The extracts were transferred into 25 mL rubber cap glass tubes, then frozen and lyophilised to complete dryness. Subsequently, the lyophilised extracts were dissolved in 2.7 ml of 0.25 mol L^{-1} NaOH + 50 mmol L^{-1} EDTA. Next, 0.3 mL of D_2O was added and the mixture was vortexed for 5 min. After being allowed to rest for 120 min, the supernatant was separated by centrifugation, filtered (<0.45 μm) and then transferred to 5 mm NMR tubes. The NMR spectra of the liquid samples were then recorded using a ^{31}P liquid NMR spectrometer (U500, Bruker, Germany) operated at 162 MHz and 298 K. Parameters of 90° pulse width, 1024 scans, and a relaxation delay of 15 s were applied. An 85% H_3PO_4 was used as the external standard for chemical shift calibration.

X-ray powder diffraction. Hydrochar samples were ground into fine powder (<200-mesh) prior to XRD analysis, which was conducted using an X-ray diffractometer (D8 Advance, Bruker, Germany), with Cu Kα radiation (λ = 0.154 nm) generated at 40 kV per 200 mA and a scintillation counter. The data were collected in the range (2θ) of 10° to 70° with a scan step of 0.02°. Finally, the minerals in the samples were identified using XRD data analysis software (MDI JADE 5.0).

Statistical analysis

Because both the temperature and retention time affected the P solid–liquid distribution, a reaction severity model was used to facilitate the description of the hydrothermal carbonisation process. The severity factor was proposed by Overend and Chornet (1987),[11] modeling the effects of the main operational variables by pseudo first-order kinetics, as shown in eqn (3):

$$R_0 = \int_0^t \exp\left[\frac{T - T_{\mathrm{ref}}}{\omega}\right] \mathrm{d}t, \tag{3}$$

where t (min) represents the residence time, T (°C) is the reaction temperature, ω is the empirical parameter related to the activation energy, assuming pseudo first-order kinetics and describing the effect of temperature. Jung and Kruse (2017) adjusted the severity factor, as shown in eqn (4), for the hydrothermal carbonization, where 100 is the temperature of reference and ω is 14.5.[13]

$$R_0 = t \exp\left[\frac{T - T_{\mathrm{Ref}}}{\omega}\right]. \tag{4}$$

The models used to fit and predict the yields of solid-P in hydrochars and inorganic-P in aqueous samples consisted of a coalification model (eqn (5)), linear regression model (eqn (6)), severity factor model (eqn (7)), and dose–response model (eqn (8)).[13]

$$P = \ln a + b \ln(t) - \frac{c}{T} + d \cdot S, \tag{5}$$

$$P = a \cdot T + b \cdot t + c \cdot S + d, \tag{6}$$

$$P = a \ln(R_0) + b \cdot S + d, \tag{7}$$

$$P = a + \frac{b - a}{1 + 10^{(c - \ln(R_0))}} + d \cdot S, \tag{8}$$

where t (min) represents the residence time, T (°C) is the reaction temperature and S is the solid ratio.

Estimation of the parameters was performed using the statistical analysis software MATLAB 2017a (MathWorks, Natick, MA, USA) and OriginPro 2017C. Validation of the prediction by the model was evaluated based on its MAE (eqn (9)):

$$\mathrm{MAE} = \frac{\sum |y_{\mathrm{i}} - \hat{y}_{\mathrm{i}}|}{n}, \tag{9}$$

where y_{i} is the measured value, $\hat{y}_{\mathrm{i}}$ is the value calculated or predicted by the model and n is the number of observations.

Conclusions

By increasing the severity of the exogenous conditions, P states were transformed from insoluble to soluble, and then repolymerised. The ^{31}P NMR spectra confirmed that the amount of organic P species initially increased with increasing reaction severity, and then decreased. These findings indicate that the hydrothermal reaction is beneficial for the homogenisation of P. Upon increasing the reaction severity, crystallisation was

hampered and the formation of amorphous carbon was enhanced. Thus, the facilitation of P reclamation might be related to sorption by the hydrochar. Investigations of the effects of endogenous Ca^{2+} on P solid–liquid distribution showed a threshold of calcium content limiting the combination of Ca and P, below which it was difficult for significant quantities of insoluble phosphates to form. Calcium ions mainly reacted with P in the form of hydroxyapatite and octacalcium phosphate. Modelling and predictions showed that the coalification model gave a good fit (R_{SP}^2 = 0.9205 and R_{IP}^2 = 0.8559) for changes in the concentration of solid total P and liquid inorganic P as well as a good prediction level (MAE_{SP} = 0.74 mg g^{-1} and MAE_{IP} = 0.62 mg g^{-1}). Overall, the results of the investigation improved the understanding of the P solid–liquid transformation mechanism under the hydrothermal reaction conditions, and from the views of external and internal hydrothermal treatment conditions, it may provide a technical support for enhancing the efficient recycling of the valuable nutrients from the swine manure. Also, it provided modelling as a new viewpoint for the study of phosphorus liquid–solid transformation, which revealed that modelling can be a quantitative method to predict the phosphorus liquid–solid distribution during hydrothermal treatment. Therefore, the study may facilitate the development of green chemistry and environment engineering.

Conflicts of interest

There are no conflicts to declare.

Acknowledgements

We thank all the anonymous reviewers for their helpful suggestions on the quality improvement of our paper. The research was sustained by the grant from the National Key Technology Research and Development Program of China (Grant number 2017YFD0800202) and the National Natural Science Foundation of China (Grant Number 31401944). Minor parts are funded by the Deutsche Forschungsgemeinschaft (DFG, German Research Foundation) – 328017493/GRK 2366 (Sino-German International Research Training Group AMAIZE-P) and Bio-SuPex (Federal Ministry of Education and Research (BMBF), 031B0606).

Notes and references

1 U. Ekpo, A. B. Ross, M. A. Camargo-Valero and L. A. Fletcher, *Bioresour. Technol.*, 2016, **214**, 637–644.
2 S. M. Heilmann, J. S. Molde, J. G. Timler, B. M. Wood, A. L. Mikula, G. V. Vozhdayev, E. C. Colosky, K. A. Spokas and K. J. Valentas, *Environ. Sci. Technol.*, 2014, **48**, 10323–10329.
3 R. Karunanithi, A. A. Szogi, N. Bolan, R. Naidu, P. Loganathan, P. G. Hunt, M. B. Vanotti, C. P. Saint, Y. S. Ok and S. Krishnamoorthy, *Phosphorus Recovery and Reuse from Waste Streams. Advances in agronomy*, Academic Press, 2015, vol. 131, pp. 173–250.
4 A. A. Szogi, M. B. Vanotti and P. G. Hunt, *J. Environ. Manage.*, 2015, **157**, 1–7.
5 P. J. A. Withers, J. J. Elser, J. Hilton, H. Ohtake, W. J. Schipper and K. C. Dijk, *Green Chem.*, 2015, **17**, 2087–2099.
6 T. T. Qian and H. Jiang, *ACS Sustainable Chem. Eng.*, 2014, **2**, 1411–1419.
7 L. C. Dai, F. R. Tan, B. Wu, M. X. He, W. G. Wang, X. Y. Tang, Q. C. Hu and M. Zhang, *J. Environ. Manage.*, 2015, **157**, 49–53.
8 T. Zhang, X. Y. He, Y. X. Deng, C. W. D. Tsang, R. F. Jiang, G. C. Becker and A. Kruse, *Sci. Total Environ.*, 2020, **698**, 134240.
9 R. Huang and Y. Tang, *Water Res.*, 2016, **100**, 439–447.
10 A. Funke and F. Ziegler, *Biofuels, Bioprod. Biorefin.*, 2010, **4**, 160–177.
11 R. P. Overend and E. Chornet, *Philos. Trans. R. Soc., A*, 1987, **321**, 523–536.
12 K. U. Suwelack, D. Wüst, P. Fleischmann and A. Kruse, *Biomass Convers. Biorefin.*, 2016, **6**, 151–160.
13 D. Jung and A. Kruse, *J. Anal. Appl. Pyrolysis*, 2017, **127**, 286–291.
14 K. Wiedner, C. Naisse, C. Rumpel, A. Pozzi, P. Wieczorek and B. Glaser, *Org. Geochem.*, 2013, **54**, 91–100.
15 A. Dieguez-Alonso, A. Funke, A. Anca-Couce, A. G. Rombola, G. Ojeda, J. Bachmann and F. Behrendt, *Energies*, 2018, **11**, 496.
16 B. J. Cade-Menun, *Talanta*, 2005, **66**, 359–371.
17 F. Kizewski, Y. T. Liu, A. Morris and D. Hesterberg, *J. Environ. Qual.*, 2011, **40**, 751–766.
18 B. E. Rittmann, B. Mayer, P. Westerhoff and M. Edwards, *Chemosphere*, 2011, **84**, 846–853.
19 S. M. Kang, X. H. Li, J. Fan and J. Chang, *Ind. Eng. Chem. Res.*, 2012, **51**, 9023–9031.
20 C. R. Bhattacharjee, S. B. Paul, A. Nath, P. P. N. Choudhury and S. Choudhury, *Materials*, 2009, **2**, 345–352.
21 S. Q. Guo, X. Y. Dong, T. T. Wu, F. Shi and C. X. Zhu, *J. Anal. Appl. Pyrolysis*, 2015, **116**, 1–9.
22 L. Yu, C. Falco, J. Weber, R. J. White, J. Y. Howe and M. M. Titirici, *Langmuir*, 2012, **28**, 12373–12383.
23 D. Licursi, C. Antonetti, S. Fulignati, S. Vitolo, M. Puccini, E. Ribechini, L. Bernazzani and A. M. R. Galletti, *Bioresour. Technol.*, 2017, **244**, 880–888.
24 C. A. Melo, F. H. S. Junior, M. C. Bisinoti, A. B. Moreira and P. F. Odair, *Waste Biomass Valorization*, 2017, **8**, 1139–1151.
25 K. S. Ro, K. B. Cantrell, P. G. Hunt, T. F. Ducey, M. B. Vanotti and A. A. Szogi, *Bioresour. Technol.*, 2019, **100**, 5466–5471.
26 R. Huang and Y. Tang, *Environ. Sci. Technol.*, 2015, **49**, 14466–14474.
27 L. C. Dai, B. Yang, H. Li, F. R. Tan, N. M. Zhu, Q. L. Zhu, M. X. He, Y. Ran and G. Q. Hu, *Bioresour. Technol.*, 2017, **243**, 860–866.

28 L. Lardon, A. Helias, B. Sialve, J. P. Steyer and O. Bernard, *Environ. Sci. Technol.*, 2009, **43**, 6475–6481.
29 H. Lu, W. Zhang, S. Wang, L. Zhuang, Y. Yang and R. Qiu, *J. Anal. Appl. Pyrolysis*, 2013, **102**, 137–143.
30 S. M. Kang, X. H. Li, J. Fan and J. Chang, *Renewable Sustainable Energy Rev.*, 2013, **27**, 546–558.
31 M. T. Reza, W. Yan, M. H. Uddin, J. G. Lynam, S. K. Hoekman, C. J. Coronella and V. R. Vásquez, *Bioresour. Technol.*, 2013, **139**, 161–169.
32 T. Karayildirim, A. Sinag and A. Kruse, *Chem. Eng. Technol.*, 2008, **31**, 1561–1568.
33 S. K. R. Patil and C. R. F. Lund, *Energy Fuels.*, 2011, **25**, 4745–4755.
34 A. Kruse and R. Grandl, *Chem. Ing. Tech.*, 2015, **87**, 449–456.
35 E. Dinjus, A. Kruse and N. Tröger, *Chem. Eng. Technol.*, 2011, **34**, 2037–2043.
36 J. G. Lynam, M. T. Reza, V. R. Vasquez and C. J. Coronella, *Fuel*, 2012, **99**, 271–273.
37 APHA (American Public Health Association), *Standard Methods for the Examination of Water and Wastewater*, Washington DC, USA, 2012.